Biochemical and Biophysical Research Communications 430 (2013) 1060–1065

Contents lists available at SciVerse ScienceDirect

Biochemical and Biophysical Research Communications

journal homepage: www.elsevier.com/locate/ybbrc

Structural–functional insights of single and multi-domain *Capsicum annuum* protease inhibitors

Manasi Mishra, Rakesh S. Joshi, Sushama Gaikwad, Vidya S. Gupta, Ashok P. Giri *

Plant Molecular Biology Unit, Division of Biochemical Sciences, CSIR-National Chemical Laboratory, Dr. Homi Bhabha Road, Pune 411 008, MS, India

ARTICLE INFO

Article history:
Received 3 December 2012
Available online 19 December 2012

Keywords:
Potato type-II protease inhibitors
CanPI
Disulfide bonding
Circular dichroism
Protein stability

ABSTRACT

Pin-II protease inhibitors (PIs) are the focus of research interest because of their large structural–functional diversity and relevance in plant defense. Two representative *Capsicum annuum* PI genes (*CanPI-15* and *-7*) comprising one and four inhibitory repeat domains, respectively, were expressed and recombinant proteins were characterized. β-Sheet and unordered structure was found predominant in CanPI-15 while -7 also displayed the signatures of polyproline fold, as revealed by circular dichroism studies. Inhibition kinetics against bovine trypsin indicated three times higher potency of CanPI-7 ($K_i \sim 57$ μM) than -15 (~184 μM). Activity and structural stability of these CanPIs were revealed under various conditions of pH, temperature and denaturing agent. Structure prediction, docking studies with proteases and mass spectroscopy revealed the organization of multiple reactive site loops of multi domain PIs in space as well as the steric hindrances imposed while binding to proteases due to their close proximity.

1. Introduction

Proteinase inhibitors (PIs) are widely spread in nature and form complexes with proteases thereby resulting into loss of their proteolytic activity. Serine PIs are well known as plant defense proteins due to their high efficiency in inhibiting digestive proteases of feeding insects and thus imparting anti-nutritional effects on them [1–3]. The Potato inhibitor-II (Pin-II) or Pot-II family of serine PIs, predominantly found in Solanaceae is extensively studied at gene as well as protein level and its functional co-relation to insect defense has been established [4]. The striking feature of Pin-II PIs is the presence of variable number of inhibitory repeat domains (IRDs) (1–8) forming multi-domain precursor proteins. A conserved Pin-II PI protein consists of an endoplasmic reticulum signal peptide of 25 amino acids (aa) followed by variable number of IRDs of ~50 aa which are separated by 5 aa long linkers. The sequence of IRDs is highly variable; however, the presence of eight cysteines, a single proline residue and an active site either for trypsin or chymotrypsin inhibition is conserved throughout IRDs. The cysteines are involved in formation of four disulfide bonds, which stabilize the repeat structure [5,6].

The three-dimensional structures of several Pin-II PIs, single- as well as two-domain, have been determined either by X-ray crystallography or NMR and these give a good outline of the structure and dynamics of this class [5,7–10]. However, there have been few studies on multi-domain inhibitors giving insights into their domain orientations, binding to proteases and stoichiometry [5,11]. Possibly because the precursors PIs are processed at linker region(s) by plant endogenous proteases to release IRD(s) [11], it has been difficult to characterize the multi-domain inhibitors from natural plant sources.

Capsicum annuum Pin-II PIs (CanPIs), displaying high isoform diversity with PIs of 1- to 4-IRDs, have been isolated and characterized to assess their defense potential against Lepidopteran proteases [2,12]. In the present study, single domain CanPI-15 (1-IRD) and four-domain CanPI-7 (4-IRD) were characterized for their protease inhibitory specificity and inhibition kinetics was studied to evaluate binding. Transitions in the structure of rCanPIs under varying conditions were monitored using biophysical techniques. CD spectroscopy, structure prediction and docking studies rendered insight into the conformational stability and/or flexibility, structure and binding mechanisms of multi-domain Pin-II PIs, respectively. We report biochemical and structural reasons for better efficiency of multi-domain inhibitors against target proteases and their high stability imparted by disulfide bonds assigning them key role in insect control strategies.

2. Materials and methods

2.1. Cloning, recombinant expression and purification of CanPIs

The cDNAs encoding the mature peptide region of *CanPIs* (*CanPI-15* and *-7*) were cloned in ligation-independent cloning

Abbreviations: CanPIs, *C. annuum* proteinase inhibitors; CD, circular dichroism; CI, chymotrypsin inhibition; IRDs, inhibitory repeat domains; MRE, mean residual ellipticity; PI, proteinase inhibitor; TI, trypsin inhibition.

* Corresponding author. Fax: +91 0 20 25902648.
E-mail address: ap.giri@ncl.res.in (A.P. Giri).

0006-291X/$ - see front matter © 2012 Elsevier Inc. All rights reserved.
http://dx.doi.org/10.1016/j.bbrc.2012.12.038

(LIC) compatible expression vector pMCSG7 [13] for recombinant expression in *Escherichia coli*. *E. coli* Origami B (DE3) cells were transformed with pMCSG7-CanPI-15 and pMCSG7-CanPI-7. Single recombinant *E. coli* colonies were initially grown overnight at 37 °C in 10 ml LB medium supplemented with antibiotics (Ampicillin, Kanamycin, and Tetracycline). The pre-culture was used to inoculate 1 L 'Terrific Broth' (TB) medium with appropriate antibiotics and allowed to grow until the OD (600 nm) reached 0.6–0.8. Cells were induced with IPTG (0.5 mM) overnight at 21 °C and harvested by centrifugation.

The cell pellet was solubilized in ice cold cell lysis buffer A (50 mM Tris–HCl, pH 8.0; 300 mM NaCl; 2% glycerol) and disrupted by sonication (0.5 s pulse with 0.5 s intervals for 10 min) using an Ultrasonic Disruptor UD-201 (Tomy, Tokyo). The supernatant and pellets were separately collected by centrifugation for 45 min at 10,000×*g*, 4 °C (RS-4S rotor, Kubota). The supernatant was loaded on Ni–NTA resin (Qiagen, Valencia, CA, USA) and purified using standard affinity chromatography. The fusion protein was eluted with buffer B (50 mM Tris–HCl, pH 8.0; 300 mM NaCl; 2% glycerol; 250 mM imidazole). The His-tag was cleaved using *Tobacco etch virus* (TEV) protease at a protease to target protein ratio of 1:100 (w/w) at RT for 12 h. Additional Ni–NTA purification was performed to remove the cleaved tag and collect the protein in flow through. This was applied on Sephadex S-75 for further purification.

2.2. Inhibitory activity assays and kinetic analysis

Inhibitory assays using rCanPIs against bovine trypsin (50 mM) were performed using chromogenic substrate Benzoyl-L-arginyl-*p*-nitroanilide (BA*p*NA) as detailed in Tamhane et al. [14]. Michaelis–Menton constant (K_m) for trypsin was calculated by using various concentrations of BA*p*NA substrate (1–5 mM). Kinetic properties of rCanPIs were analyzed over a range of concentration of inhibitors (100–1000 μM). IC_{50} and K_i values for each inhibitor were calculated from the sigmoid curve and Cheng–Prusoff's classical equation, respectively [15]:

$$K_i = IC_{50}/(1 + [S]/K_m)$$

2.3. Fluorescence measurements and ANS binding studies

The rCanPI protein samples (100 μg/ml) were incubated in an appropriate buffer over the pH range of 2–10 for 4 h at 28 °C. The following buffers (25 mM) were used for these studies: Glycine–HCl for pH 1–3, acetate for pH 4–5, phosphate for pH 6–7, Tris–HCl for pH 8–9 and Glycine–NaOH for pH 10–12. Appropriate aliquots from samples were used to check for TI activity and fluorescence measurements for binding with 1-anilino-8-naphthalenesulfonate (ANS) were performed on Perkin Elmer LS 50B luminescence spectrometer at 28 °C. ANS is a hydrophobic dye which binds to solvent-exposed hydrophobic regions in a protein and shows increased fluorescence intensity and blue shift in the λ_{max} of emission [16]. The final ANS concentration used was 50 μM, excitation wavelength was 375 nm and total fluorescence emission was monitored between 400 and 550 nm. Slit widths of 7 nm each were set for excitation and emission monochromators and the spectra were recorded at 100 nm/min. Reference spectrum of ANS in the buffer was subtracted from the spectrum of the sample.

2.4. Circular dichroism (CD) measurements

The far UV CD spectra (in wavelength range of 195–300 nm) of rCanPI proteins (125 μg/ml) were recorded on a J-815 spectropolarimeter (Jasco, Tokyo, Japan) at 28 °C in a quartz cuvette. Each

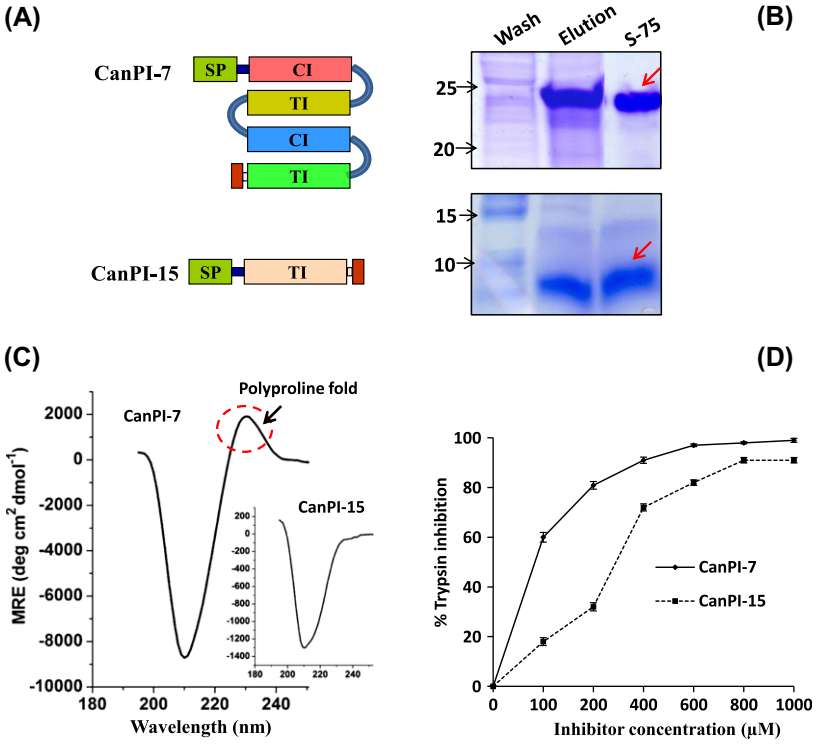

Fig. 1. (A) Diagrammatic representation of the gene structure of two *CanPIs* from *C. annuum*, with their signal peptide (SP), various IRD(s), linker region(s) and the stop codon. The IRDs varying in the aa sequence are shown in different colors. Trypsin inhibitory (TI) domains and chymotrypsin inhibitory (CI) domains are marked. (B) Purified recombinant CanPI-15 (6 kDa) and CanPI-7 (25 kDa) separated on 15% SDS–PAGE and stained with Coomassie Blue R250. Lane 1, wash with 20 mM of imidazole. Lane 2, fusion protein eluted with 250 mM of imidazole. Lane 3, purified through Sephadex-75 column. (C) Far UV CD spectra of rCanPIs. Signatures of polyproline fold observed in rCanPI-7. (D) Inhibition kinetics of CanPI-15 and -7 against bovine trypsin. The inhibition of trypsin follows a sigmoidal pattern with increasing concentration of the inhibitors.

CD spectrum was accumulated from three scans at 100 nm/min with a 1 nm slit width, cell path length 0.1 cm and nominal resolution of 0.5 nm. All spectra were corrected for buffer contributions and observed values were converted to mean residual ellipticity (MRE) in deg cm^2 $dmol^{-1}$ defined as

$$MRE = M\theta_\lambda/10dcr$$

where M is the molecular weight of the protein, θ_λ is CD in millidegree, d is the path length in cm, c is the protein concentration in mg/ml and r is the number of amino acid residues in the protein.

The rCanPI protein samples (125 μg/ml) were incubated in above mentioned buffers of varying pH and used for CD measurements. Temperature effects were monitored by incubating the protein samples in the temperature range of 24–99 °C for 2 h and measuring the CD spectra. CD spectra were recorded for protein samples incubated in 0–8 M GdnHCl for 2 h.

2.5. Structure prediction and assessment for CanPIs

Structure of CanPI-15 was predicted by homology modeling, based on the ~90% sequence identity with chymotrypsin inhibitor-1 structure from Russet Burbank potato tubers at 2.1 Å resolution (PDB ID: 4SGB_I). 3D structure of CanPI-7 was obtained using the automated I-TASSER service (http://zhang-lab.ccmb.med.umich.edu/I-TASSER/) which uses multiple PDB structures depending on its structural conservation, to model different parts of protein [17–19]. The best model selected from output based on C-score was subjected to an energy minimization procedure with GROMOS96 (The PyMol Molecular Graphics System, Version 1.2r3 pre, Schrödinger LLC.) to reduce poor Van der Waals contacts and correct the stereochemistry of the model. The quality of the model produced was assessed by checking the protein stereology using the PROCHECK and the energy was checked by ProSA.

2.6. Macromolecular docking of CanPI-7 with proteases

Docking study was conducted to evaluate the binding conformation and interaction of CanPI-7 with trypsin and chymotrypsin. Models of CanPI-7 and bovine trypsin (PDB ID: 1S0Q) and chymotrypsin (PDB ID: 1YPH) were submitted separately to online server GRAMMX [20] following the standard protocols. Successively, two trypsin and two chymotrypsin molecules were docked and analyzed to study the probable mechanism of binding.

2.7. MALDI-TOF-MS analysis of protease-PI complex

Equimolar amounts of rCanPI-7 and trypsin were mixed and incubated for 20 min at 37 °C. The mass spectral analysis of the reaction mix was done on Q-TOF-MALDI-TOF-MS with a standard instrumental protocol (High Definition Mass spectrometer, Waters Corporation, Milford, MA, USA). Sample preparation, spectral acquisition and processing were done as described earlier [12].

3. Results and discussion

3.1. Recombinant expression of CanPIs

The diagrammatic representation of the selected single (*CanPI-15*) and multi-domain (*CanPI-7*) PI genes from *C. annuum* and sequence alignments of the constituent five unique IRDs are shown in Fig. 1A and Suppl. Fig. 1, respectively. CanPI-15 comprised a single trypsin inhibitory domain (TI) while CanPI-7 had two TI and two chymotrypsin inhibitory (CI) domains. The core reactive site of an IRD, 'PKN' or 'PRN' for TIs and 'TLN' for CIs confined by two conserved cysteine residues is marked (Suppl. Fig. 1).

CanPIs being disulfide rich proteins, we chose *E. coli* Origami B (DE3) as a host to produce the recombinant proteins [21,22]. Origami B (DE3) is a modified strain that has mutations in both, the thioredoxin reductase (trxB) and glutathione reductase (gor) genes thus maintaining a non-reducing condition in cytoplasm facilitating the S–S bond formation in the recombinant protein in the proper order. The soluble fraction was purified and final preparations yielded single protein corresponding to 6 kDa for CanPI-15 and 25 kDa for CanPI-7 (Fig. 1B).

CD Pro analysis of the far UV CD spectrum (Fig. 1C) yielded the values of secondary structure elements as: α-helix-3.8%, β-sheet-41.4%, turns-21.2% and unordered-33.4% for CanPI-15. The single negative band between 208- and 210-nm and the CDPro analysis validated that the CanPIs were β-sheet rich and unordered proteins in accordance to the earlier structural reports on Pin-II PIs [5–9]. Interestingly, CanPI-7 exhibited signatures of a polyproline fold (PPII) structure, bearing a small positive band near 227 nm and a large negative band between 208- and 210-nm with a cross over at 223 nm. Typically this kind of structure is adapted by proteins rich in proline/hydroxyproline but, even sequences not rich in proline can also take up this structure [23,24]. Earlier, several residues with PPII structure within the long unordered loops in Bowman-

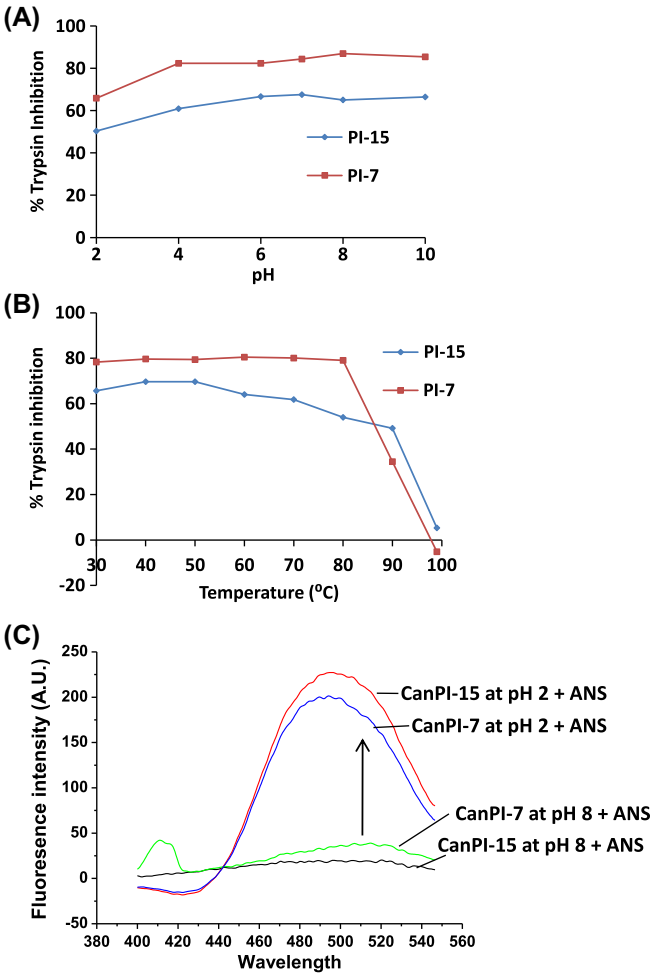

Fig. 2. rCanPIs under varying pH and temperature. (A) Percent inhibition of bovine trypsin by rCanPIs incubated for 4 h in buffers of pH 2–10. (B) Percent inhibition of bovine trypsin by rCanPIs incubated for 2 h at temperatures 24–99 °C. (C) ANS binding of rCanPIs after incubation in buffers of pH 2 and 8. Increase in ANS intensity and blue shift is observed in rCanPIs at pH 2. (For interpretation of the references to colour in this figure legend, the reader is referred to the web version of this article.)

Birk protease inhibitor have been reported by Raman optical activity spectroscopy [25].

3.2. Inhibitory activities and kinetic analysis of CanPIs

Kinetic studies revealed stronger inhibition of trypsin by CanPI-7 (IC_{50}, 89 μM) than CanPI-15 (IC_{50}, 277 μM). The inhibition of trypsin followed a sigmoidal pattern with increasing concentrations of the inhibitors (Fig. 1D). CanPI-7 with low K_i (~57.42 μM) turned out to be a more potent inhibitor and indicated more 'tight binding' than CanPI-15 ($K_i \sim 184.66$ μM). CanPI-7 attained higher inhibition of bovine trypsin at 3-fold lower concentrations than CanPI-15. This highlights the exponential inhibitory effects that could be attained by use of multi domain PIs against proteases.

3.3. Stabilities of CanPI-15 and -7 to pH, temperature and denaturing agents

CanPI-15 and -7 showed structural stability over a wide range of pH conditions (pH 2–10) while pH 7–8 was the optimum range for inhibitory activity (Fig. 2A). CanPIs exhibited ~10% loss of inhibitory activity at acidic pH 2. The ellipticity and the minima at 210 nm, for both rCanPIs at pH 2 and 8, remained unaltered indicating no loss of the native secondary structure (Fig. 3A and B). Further, the rCanPIs checked for ANS binding to look for any partial unfolding of the proteins under acidic pH conditions showed two times increase in fluorescence intensity at pH 2 (Fig. 2C) with blue shift of λ_{max} to 500 nm indicating exposure of hydrophobic patches on the surface of the protein. However, this alteration in the structure did not seem to affect the activity.

CanPI-7 retained its inhibitory activity even after incubation at 80 °C for 2 h while CanPI-15 began to gradually lose its activity starting from 60 °C (Fig. 2B). At higher temperatures, beyond 90 °C both the proteins displayed progressive loss of activity resulting in to complete denaturation. In accordance to the retained activity, both the CanPIs showed 15–25% gradual loss of secondary structure only from 70 °C to 90 °C (Fig. 3C and D). The decrease in the positive band at 227 nm observed with increasing temperature supported the assignment of PPII fold in CanPI-7 (Fig. 3D). The high thermo stability of CanPIs can be ascribed to the presence of disulfide bonds. The unusual heat resistance of various proteins has been attributed to the presence of cysteines resulting in intra-domain or inter-domain disulfide bonds [26,27].

Both, CanPI-15 and -7 showed apparently 50% loss of secondary structure in presence of GdnHCl from 5 M to 8 M concentration as indicated by the loss of ellipticity at 210 nm (Fig. 3E and F). CD spectra of CanPI-15 showed positive band at 227 nm with higher concentrations of GdnHCl indicating the formation of polyproline fold (Fig. 3E). This implied that although CanPI-15 did not show any indication of PPII fold in its native CD profile, it is prone to adapt such kind of structure under specific conditions. CanPI-7 also displayed an increase in the positive band at progressively higher GdnHCl concentrations supporting the earlier hypothesis that formation of PPII like structure is promoted in presence of denaturing agent [26]. This structural rearrangement is unique and has been observed in very few proteins like Human tropoelastin, Titin, and Bowman-Birk inhibitor [24,25].

3.4. Structure prediction for CanPIs

Predicted structure of single domain CanPI-15 was found to be similar with NMR structure of *Nicotiana alata* trypsin inhibitor (1TIH) and forms complex with a single molecule of trypsin [28]. For CanPI-7, we had used *de novo* protein modeling approach due to absence of X-ray crystallographic or NMR structure of any four domain Pin-II PI molecule. I-TASSER used various PDB structures like 1fybA, 1pjuA and 1oyvI to model specific parts of the query molecule, all these PDB(s) belonged to structure of Pin-II PIs. The selected best model (Fig. 4A) had C score of −3.83, Tm score = 0.35 ± 0.12 and RMSD = 13.4 ± 4.0 Å which are within the acceptable range for molecular modeling. β-Sheets and unordered loops were the major secondary structures of CanPI-7. This model represented the four solvent exposed reactive sites (RL1–RL4) lying on unordered loops as shown in Fig. 4A. RL1 and RL2 were in close

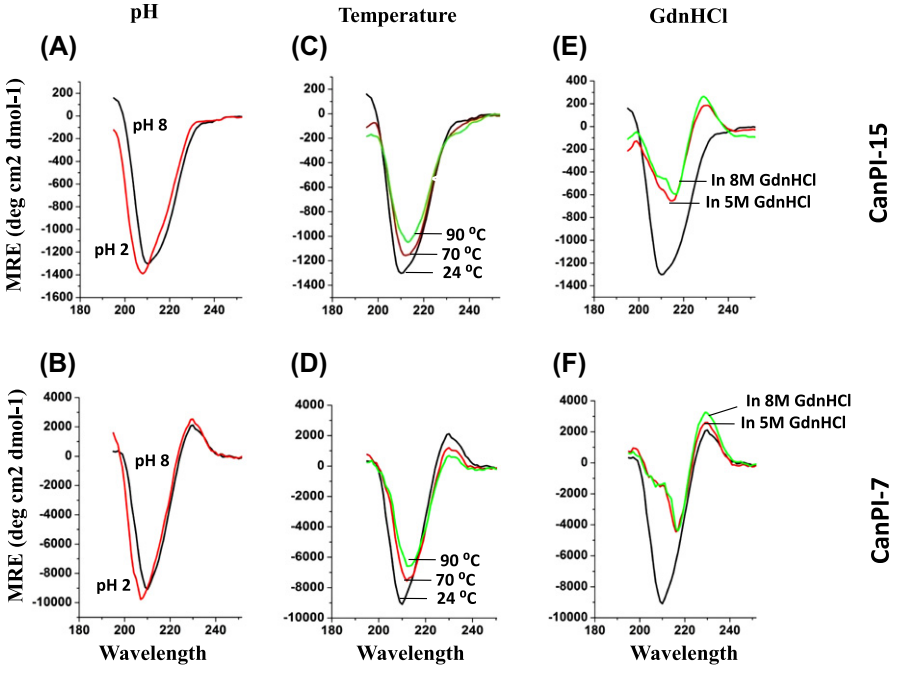

Fig. 3. Far UV CD spectra of rCanPI-15 and -7. (A, B) Incubated in buffers of pH 2 and 8. (C, D) Incubated at varying temperatures. Loss of secondary structure is observed with increase in temperature. (E, F) 5 M and 8 M GdnHCl treated rCanPIs. Polyproline fold formation was observed in CanPI-15 in presence of GdnHCl. Fifty percent residual secondary structure is observed for both the rCanPIs in presence of 8 M GdnHCl.

proximity with a distance of 21 Å while RL3 and RL4 appeared distant with 48 Å distance. Earlier structural studies on Pin-II PIs had been limited to two-domain precursors from tomato [10] and have shown the orientation of the two domains directly facing each other leading to binding with two protease molecules independently. In case of multi domain PIs, the role of interdomain interactions has been speculated as a key determinant of orientations of the domains relative to each other [5]. The presence of 2–6 TI domains in many Pin-II PIs has suggested the functional significance of the combination of IRDs within a single PI. It was intriguing to speculate about the orientation and binding of the four domain inhibitor as in case of CanPI-7. PROCHECK and ProSA analysis, also validated that the modeled structure ID was acceptable for the further analysis (Suppl. Fig. 2).

3.5. Probable mechanism of CanPI-7 binding with multiple target protease molecules

The goal of the initial stage of docking is to generate as many near-native complex structures as possible. Four complexes (Complex 1 to Complex 4) (Fig. 4B) were obtained from multiple docking analysis with four trypsin molecules. Complex 1 showed the close proximity of trypsin molecule with the first reactive loop (RL1) with distance of 4.6 Å between Cα atom of central residue of RL1 and Ser195 of trypsin. Binding of the first trypsin molecule at RL1, caused the steric hindrance for binding of the next trypsin molecule at second reactive loop (RL2) due to their close proximity. However, the further two trypsin molecules showed close proximity with third (RL3) and fourth (RL4) reactive loops with

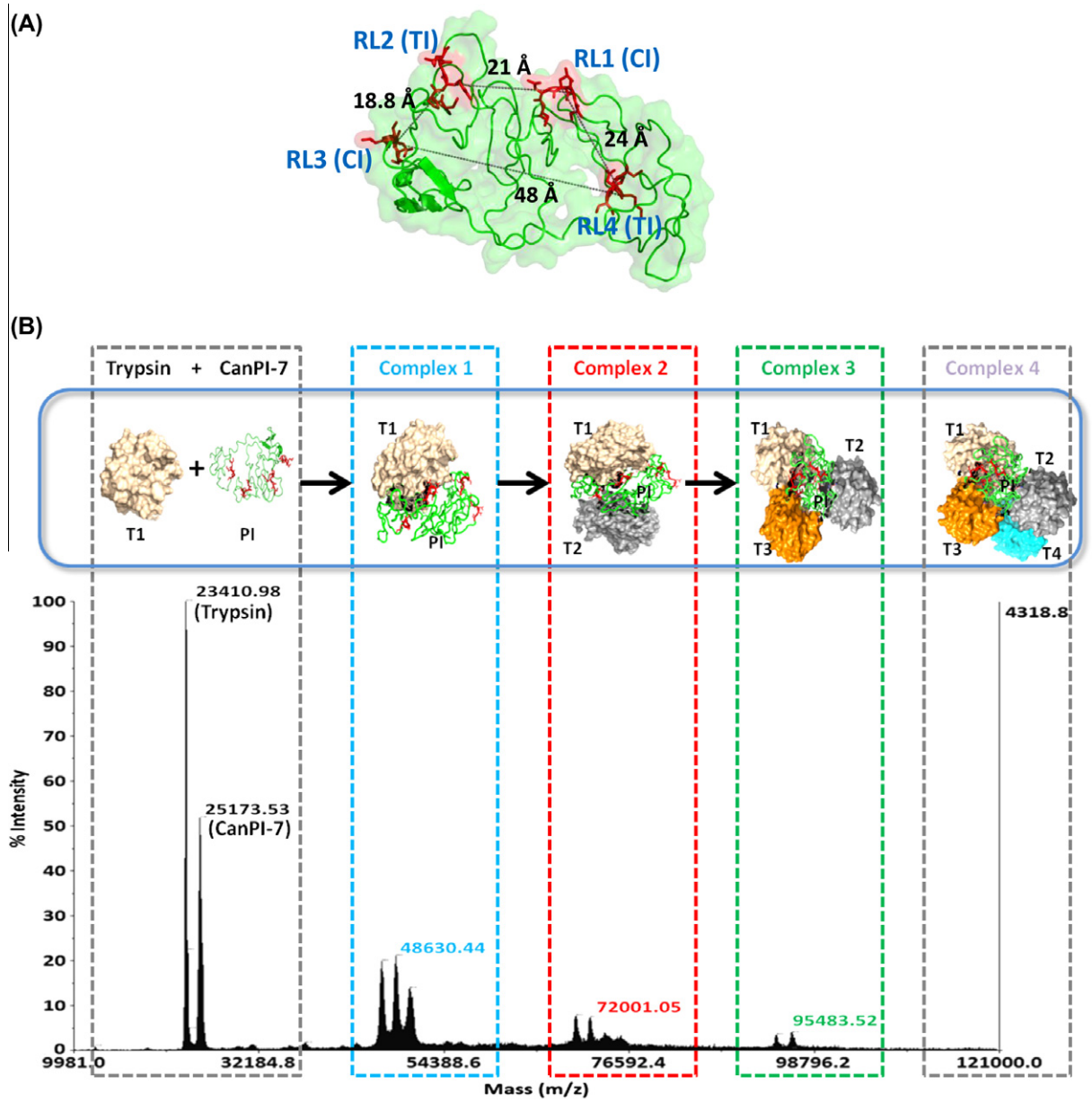

Fig. 4. Structure and binding of CanPI-7 with proteases. (A) The predicted structure of CanPI-7 from I-TASSER server displayed β-sheets and unordered loops as the major secondary structural components and the four reactive sites displayed in red color (RL1–RL4) lied on exposed loops. CI and TI specificity of the reactive loops and the distances between the active site loops are marked. (B) Binding of CanPI-7 (shown in green color) with four molecules of trypsin (T1, T2, T3 and T4) shown with brown, gray, orange and blue colors, respectively. In docking, close proximity to RSL 1, 3 and 4 was observed with trypsin molecules while binding to RSL2 appeared obstructed because of steric hindrance. MALDI-TOF-MS spectra displayed formation of bi, tri and tetravalent complex of CanPI-7 with trypsin molecules while peak corresponding to pentavalent complex of CanPI-7 bound to four trypsin molecules could not be detected.

intermolecular distances of 8.1 Å and 10.4 Å, respectively. The static complex of CanPI-7 representing at least three protease molecules in close proximity to the RLs, supports its higher potency corroborating with the enzymatic assays. The peaks corresponding to bi (48,630 Da), tri (72,001 Da) and tetravalent (95,483 Da) complexes in mass spectral analysis (Fig. 4B) further confirmed the predicted binding hypothesis. However, it is likely that both, the bound and unbound forms of CanPI-7 could exhibit conformational flexibility within the domains relative to each other or in reactive site loops, leading to either strong interaction with more number of protease molecules or lesser than those observed in the static model of the complex. Molecular dynamic simulations of each of the complexes or crystal structures would deliver the dynamic picture of this interaction. Cross reactivity in binding of trypsin or chymotrypsin molecules to either TI or CI sites was also observed (Fig. 4B and Suppl. Fig. 3) and suggests that the reactive site loops retain adequate conformational flexibility to allow recognition by a variety of protease molecules. PIs being an innate part of the plant defense strategies protecting them from insects, fungi and bacteria must have enough variability to interact with a wide range of proteases they come across.

Acknowledgments

The Council of Scientific and Industrial Research (CSIR), Government of India, New Delhi supported this project under network project grants to CSIR-National Chemical Laboratory, Pune (NWP0003). MM and RSJ acknowledge CSIR for research fellowships. MM acknowledge DAAD for 'Short term scholarship' to work at EMBL, Hamburg, Germany and Dr. Jochen Muller Deickmann, EMBL, Hamburg for his academic guidance and critical inputs in the manuscript. Authors acknowledge Dr. Saravanan Pannerselvam from EMBL for help in cloning and expression; Sonali Rohamare from NCL, Pune for help in fluorescence spectroscopy; Dr. H.N. Gopi from IISER, Pune for providing instrument for CD spectroscopy.

Appendix A. Supplementary data

Supplementary data associated with this article can be found, in the online version, at http://dx.doi.org/10.1016/j.bbrc.2012.12.038.

References

[1] A.P. Giri, N.P. Chougule, M.A. Telang, V.S. Gupta, Engineering insect tolerant plants using plant defensive proteinase inhibitors, Recent Res. Dev. Phytochem. 8 (2005) 117–137.
[2] V.A. Tamhane, A.P. Giri, M.N. Sainani, V.S. Gupta, Diverse forms of Pin-II family proteinase inhibitors from *Capsicum annuum* adversely affect the growth and development of *Helicoverpa armigera*, Gene 403 (2007) 29–38.
[3] M. Hartl, A.P. Giri, H. Kaur, I.T. Baldwin, Serine protease inhibitors specifically defend *Solanum nigrum* against generalist herbivores but do not influence plant growth and development, Plant Cell 22 (2010) 4158–4175.
[4] T.R. Green, C.A. Ryan, Wound-induced proteinase inhibitor in plant leaves: a possible defense mechanism against insects, Science 175 (1972) 776–777.
[5] H.J. Schirra, D.J. Craik, Structure and folding of potato type II proteinase inhibitors: circular permutation and intramolecular domain swapping, Protein Pept. Lett. 12 (2005) 421–431.
[6] H.J. Schirra, M.A. Anderson, D.J. Craik, Structural refinement of insecticidal plant proteinase inhibitors from *Nicotiana alata*, Protein Pept. Lett. 15 (2008) 903–909.
[7] H.M. Greenblatt, C.A. Ryan, M.N.G. James, Structure of the complex of *Streptomyces griseus* proteinase B and polypeptide chymotrypsin inhibitor-1 from Russet Burbank potato tubers at 2.1 Å resolution, J. Mol. Biol. 205 (1989) 201–228.
[8] K.J. Nielsen, R.L. Heath, M.A. Anderson, D.J. Craik, The Three-dimensional solution structure by H NMR of a 6-kDa proteinase inhibitor isolated from the stigma of *Nicotiana alata*, J. Mol. Biol. 242 (1994) 231–243.
[9] K.J. Nielsen, R.L. Heath, M.A. Anderson, D.J. Craik, Structures of a series of 6-kDa trypsin inhibitors isolated from the stigma of *Nicotiana alata*, Biochemistry 34 (1995) 14304–14311.
[10] I.H. Barrette-Ng, K.K. Ng, M.M. Cherney, G. Pearce, C.A. Ryan, M.N. James, Structural basis of inhibition revealed by a 1:2 complex of the two-headed tomato inhibitor-II and subtilisin Carlsberg, J. Biol. Chem. 278 (2003) 24062–24071.
[11] R.L. Heath, P.A. Barton, R.J. Simpson, G.E. Reid, G. Lim, M.A. Anderson, Characterization of the protease processing sites in a multidomain proteinase inhibitor precursor from *Nicotiana alata*, Eur. J. Biochem. 230 (1995) 250–257.
[12] M. Mishra, V.A. Tamhane, N. Khandelwal, M.J. Kulkarni, V.S. Gupta, A.P. Giri, Interaction of recombinant CanPIs with *Helicoverpa armigera* gut proteases reveals their processing patterns, stability and efficiency, Proteomics 10 (2010) 2845–2857.
[13] W.H. Eschenfeldt, L. Stols, C.S. Millard, A. Joachimiak, M.I. Donnelly, A family of LIC vectors for high-throughput cloning and purification of proteins, Methods Mol. Biol. 498 (2009) 105–115.
[14] V.A. Tamhane, N.P. Chougule, A.P. Giri, A.R. Dixit, M.N. Sainani, V.S. Gupta, *In vivo* and *in vitro* effect of *Capsicum annum* proteinase inhibitors on *Helicoverpa armigera* gut proteinases, Biochim. Biophys. Acta, Gen. Subj. 1722 (2005) 156–167.
[15] Y.C. Cheng, W.H. Prusoff, Relationship between the inhibition constant (K_i) and the concentration of inhibitor which causes 50 per cent inhibition (I_{50}) of an enzymatic reaction, Biochem. Pharmacol. 22 (1973) 3099–3108.
[16] G.V. Semisotnov, N.A. Rodionova, O.I. Razgulyaev, V.N. Uversky, A.F. Gripas, R.I. Gilmanshin, Study of the 'molten globule' intermediate state in protein folding by a hydrophobic fluorescent probe, Biopolymers 31 (1991) 119–128.
[17] Y. Zhang, I-TASSER server for protein 3D structure prediction, BMC Bioinform. 9 (2008) 40.
[18] A. Roy, A. Kucukural, Y. Zhang, I-TASSER: a unified platform for automated protein structure and function prediction, Nat. Protoc. 5 (2010) 725–738.
[19] A. Roy, D. Xu, J. Poisson, Y. Zhang, A protocol for computer-based protein structure and function prediction, J. Visualized Exp. 57 (2011) e3259.
[20] A. Tovchigrechko, I.A. Vakser, GRAMM-X public web server for protein–protein docking, Nucleic Acids Res. 34 (2006) W310–W314.
[21] M. Venturi, C. Seifert, C. Hunte, High level production of functional antibody fab fragments in an oxidizing bacterial cytoplasm, J. Mol. Biol. 315 (2002) 1–8.
[22] S. Xiong, Y. Wang, X. Rong Ren, B. Li, M.Y. Zhang, Y. Luo, L. Zhang, Q.L. Xie, K.Y. Su, Solubility of disulfide-bonded proteins in the cytoplasm of *Escherichia coli* and its "oxidizing" mutant, World J. Gastroenterol. 11 (7) (2005) 1077–1082.
[23] M.A. Young, E.S. Pysh, Vacuum ultraviolet circular dichroism of poly(L-proline) I and II, J. Am. Chem. Soc. 97 (18) (1975) 5100–5103.
[24] B. Bochicchio, A.M. Tamburro, Polyproline II structure in proteins: identification by chiroptical spectroscopies, stability, and functions, Chirality 14 (2002) 782–792.
[25] E. Smyth, C.D. Syme, E.W. Blanch, L. Hecht, M. Vasak, L.D. Barron, Solution structure of native proteins with irregular folds from Raman optical activity, Biopolymers 58 (2001) 138–151.
[26] R. Wetzel, L.J. Perry, W.A. Baase, W.J. Becktel, Disulfide bonds and thermal stability in T4 lysozyme, Proc. Natl. Acad. Sci. USA 85 (1988) 401–405.
[27] M. Luckey, R. Ling, A. Dose, B. Malloy, Role of a disulfide bond in the thermal stability of the LamB protein trimer in *Escherichia coli* outer membrane, J. Biol. Chem. 266 (3) (1991) 1866–1871.
[28] R.S. Joshi, M. Mishra, V.A. Tamhane, A. Ghosh, et al., The remarkable efficiency of a Pin-II proteinase inhibitor sans two conserved disulfide bonds is due to enhanced flexibility and hydrogen-bond density in the reactive site loop, J. Biomol. Struct. Dyn., http://dx.doi.org/10.1080/07391102.2012.745378.